ECOHYDROLOGY
Ecohydrol. **7**, 409–419 (2014)
Published online 1 January 2013 in Wiley Online Library
(wileyonlinelibrary.com) DOI: 10.1002/eco.1360

Quantifying transpirable soil water and its relations to tree water use dynamics in a water-limited pine forest

Tamir Klein,[1] Eyal Rotenberg,[1] Ella Cohen-Hilaleh,[1] Naama Raz-Yaseef,[1,2] Fyodor Tatarinov,[1] Yakir Preisler,[1] Jérôme Ogée,[3] Shabtai Cohen[4] and Dan Yakir[1]*

[1] *Department of Environmental Sciences and Energy Research, Weizmann Institute of Science, Rehovot, Israel*
[2] *Department of Environmental Science, Policy and Management, UC Berkeley, Berkeley, CA, USA*
[3] *INRA, UR1263 EPHYSE, F-33140, Villenave d'Ornon, France*
[4] *Institute of Soil, Water and Environmental Sciences, Volcani Center ARO, Beit Dagan, Israel*

ABSTRACT

Knowledge of the relationship between soil water dynamics and tree water use is critical to understanding forest response to environmental change in water-limited ecosystems. However, the dynamics in soil water availability for tree transpiration (T_t) cannot be easily deduced from conventional measurements of soil water content (SWC), notably because T_t is influenced by soil water potential (Ψ_s) that, in turn, depends on soil characteristics. Using tree sap flow and water potential and deriving depth-dependent soil water retention curves, we quantified the 'transpirable soil water content' (tSWC) and its seasonal and inter-annual variations in a semi-arid *Pinus halepensis* forest. The results indicated that tSWC varied in time and with soil depth. Over one growing season T_t was 57% of rain and 72% of the infiltrated SWC. In early winter, T_t was exclusively supported by soil moisture at the top 10 cm (tSWC = 11 mm), whereas in spring (tSWC > 18 mm) and throughout the dry season, source water for T_t shifted to 20–40 cm, where the maximum fine root density occurs. Simulation with the soil–plant–atmosphere water and energy transport model MuSICA supported the idea that consistent tSWC at the 20–40 cm soil layer critically depended on limited water infiltration below 40 cm, because of high water retention below this depth. Quantifying tSWC is critical to the precise estimation of the onset and termination of the growing season (when tSWC > 0) in this semi-arid ecosystem. Copyright © 2013 John Wiley & Sons, Ltd.

KEY WORDS soil water retention; water availability; hydrological budget; sap flow; water potential

Received 4 June 2012; Revised 30 September 2012; Accepted 19 November 2012

INTRODUCTION

Soil water availability is a major driver of plant productivity globally and is the limiting factor in semi-arid regions. Water limitation is predicted to increase in many regions, including the entire Mediterranean region (Christensen *et al*., 2007). Understanding the relationships between soil water dynamics and tree water use is hence essential for current as well as future forest management.

In previous studies of water availability for plant transpiration, it was noticed that transpiration is maintained until a critical (non-zero) point of soil water content (SWC) is reached (Martin 1940; Veihmeyer 1956; Ritchie 1974). Identification of this point has been addressed in several ways. Initially, Ritchie (1981) used the concept of extractable soil water content (eSWC), defined as the difference between SWC in the root zone at field capacity and at the wilting point, corresponding to a mean soil water potential (Ψ_s) of −1·5 MPa. A similar index was subsequently applied to laboratory conditions, termed available soil water content (aSWC, Reid *et al*., 1984). Using soil-drying experiments on seven sorghum crops, Robertson and Fukai (1994) found that in most situations, the transpiration rate declined once eSWC in the soil layer with maximum rooting depth declined below 30%. Similarly, Gollan *et al*. (1985) found strong reductions of stomatal conductance at about 50% eSWC in the woody shrub *Nerium oleander*. Granier *et al*. (1999) proposed another measure, i.e. the fraction of relative extractable water, defined as bulk SWC minus minimum SWC and normalized to field capacity. This approach has been subsequently used extensively (e.g. Oren *et al*., 1998; Maseyk *et al*., 2008; Domec *et al*., 2010). In addition to these three indices, the fraction of transpirable water was defined as the difference between an irrigated pot weight (i.e. at field capacity) and its weight on the day when relative transpiration rate reached 10% of maximum (Sinclair and Ludlow 1986).

In an ecological context, resolving the relationships between soil water dynamics and tree water use may require additional considerations. Firstly, soil water retention properties usually vary with depth (Breda *et al*., 1995; Oren *et al*., 1998; Granier *et al*., 1999; Warren *et al*., 2005; Domec *et al*., 2010), so that amounts of transpirable water are not necessarily homogeneously distributed. Secondly, the point of stomatal closure is species-specific (Tardieu and Simonneau 1998; Bond and Kavanagh 1999; Klein *et al*., 2011) and depends on leaf water potential rather than bulk SWC. This leads to species-specific differences in the ability to sustain transpiration under soil hydraulic limitations (Sperry *et al*., 1998; Heiskanen and Makitalo 2002). Finally, to quantify the amounts of transpirable water, one must account for the

*Correspondence to: Dan Yakir, Department of Environmental Sciences and Energy Research, Weizmann Institute of Science, Rehovot, Israel.
E-mail: dan.yakir@weizmann.ac.il

relevant soil profile, as well as the complete ecosystem water balance (Williams *et al*., 1996; Oren *et al*., 1998; Siqueira *et al*., 2008; Schwarzel *et al*., 2009).

This study was conducted at an operational research site in a semi-arid pine forest (Yatir forest, Israel; http://www.weizmann.ac.il/ESER/People/Yakir/YATIR/). Semi-arid forests can maintain relatively high productivity (Gruenzweig *et al*., 2003), associated with a range of physiological and phenological adjustments (Gruenzweig *et al*., 2007; Maseyk *et al*., 2008). A complete understanding of forest functioning under such conditions requires quantitative assessment of the relationships between soil water dynamics and plant water use. The objectives of this paper are as follows: (1) to provide quantification of transpirable water and its changes across different soil layers and along the year and (2) to test the relationships between the transpirable water amounts calculated in (1) and tree water use dynamics. Analysis of these relationships will help quantify soil water availability for tree transpiration, which will improve our understanding of the ecohydrology of semi-arid pine forests, as well as provide forestry and water management tools.

MATERIALS AND METHODS

Site description

Our study was conducted in Yatir forest, a 40-year-old *Pinus halepensis* plantation located at the northern edge of the Negev desert, Israel (31°20′N, 35°20′E). The forest covers an area of 2800 ha and lies on a predominantly light brown Rendzina soil ($79 \pm 45{\cdot}7$-cm deep), overlying a chalk and limestone bedrock. The climate is hot (40-year average mean annual temperature is 28 °C) and dry (40-year average mean annual precipitation is 285 ± 88 mm). Stand density is ~300 trees ha^{-1}, mean tree height is $10{\cdot}2 \pm 2{\cdot}49$ m and mean diameter at breast height is $19{\cdot}8 \pm 5{\cdot}61$ cm, leading to an average leaf area index of about 1·50 (Sprintsin *et al*., 2011). Surface runoff (R) and deep drainage (D) are negligible (Shachnovich *et al*., 2008; Raz-Yaseef *et al*., 2010b), and the water table is below 300 m, eliminating the possibility of groundwater recharge (S) or other sources than precipitation (P) for evapotranspiration (ET). The long-term hydrological balance between the ecosystem water components ($P = R + S + ET + D$) can therefore be simplified in Yatir to $P \approx ET$. In 2000, an instrumented flux tower was installed in the geographic centre of the forest, allowing continuous measurements of both P and ET (Rotenberg and Yakir 2010). Unless specified, all other measurements and samples were taken within the flux tower footprint.

Soil water content

Soil moisture has been measured continuously over the past 6 years using time domain reflectometry sensors (TRIME, IMKO Inc., Ettlingen, Germany). The sensors were installed horizontally in three different pits dug in three locations, 5–70 m from the flux tower, varying in depth according to the soil/bedrock structure at each location: 5, 15 and 25 cm in all pits, 50 and 70 cm in pits 1 and 3 and 125 cm in pit 1 (Raz-Yaseef *et al*., 2010a, b). Variability in soil moisture between sensors of similar depths but different locations (pits) was typically 0·005–0·021 m^3 m^{-3}, and never exceeded 0·048 m^3 m^{-3}. The range of standard errors for specific depth layers is given in the text and figure captions.

Soil mechanical arrangement

In June 2009, six uninterrupted soil samples were taken from the flux tower plot in Yatir using 53-mm rings (Eijkelkamp, Giesbeek, Netherlands). Soil mechanical arrangement and particle size distribution were analysed according to the equivalent diameter scale used by the International Soil Science Society (Marshall 1947). The analysis was carried out by the density method with variable depth, on the basis of Stock's law (Bouyoucos 1962). Approximately 40 g of oven-dried soil samples were weighted and mixed with 100-ml dispersing solution of 2·5% $Na_4P_2O_7 * 10H_2O$ (Merck chemicals, Darmstadt, Germany) and 100-ml distilled water, as described by Klute (1986). After 10 min, the suspension was transferred into a 1-l measuring tube, and the remaining volume was filled with distilled water. Suspensions were left overnight to reach equilibrium temperature, and then preliminary readings of temperature and density were taken to determine time intervals for further density measurements, using a hydrometer on well-mixed soil suspensions. Particle size distribution was determined for four depths: 0–10, 10–20, 20–40 and 40–60 cm, denoted as layers I–IV, respectively.

Soil water retention

The mechanical arrangement analysis at each depth allowed computation of discrete approximated water retention curves, describing the relationship between the soil water capillary head (Ψ) and the respective water content (SWC), as described by Gupta and Larson (1979). The approximation was carried out by the RETC software package (http://epa.gov/ada/csmos/models/retc.html) using the so-called van Genuchten–Mualem model (van Genuchten *et al*., 1991):

$$\mathrm{SWC} = \mathrm{SWCr} + \frac{\mathrm{SWCs} - \mathrm{SWCr}}{[1 + (\propto |\Psi|)^n]^m} \qquad (1)$$

where SWCr and SWCs are the residual and saturation water content, respectively, and α, n and m are the soil parameters ($m = 1 - 1/n$, $n > 1$). The robustness and accuracy of this pedo-transfer function and of the RETC software have been demonstrated at various soil types in numerous studies (e.g. Yates *et al*., 1992; Woesten *et al*., 1994; Ritter *et al*., 2004; Matula and Spongrova 2007). Errors associated with the SWC data and the retention curve estimation were calculated according to error propagation rules (Taylor 1997). If x and y have independent errors δx and δy, then the error in $z = x + y$ is $\delta z = (\delta x^2 + \delta y^2)^{1/2}$, and the error in $z = x \times y$ is $\delta z/z = ((\delta x/x)^2 + (\delta y/y)^2)^{1/2}$.

Soil water potential threshold for tree transpiration

A Ψ_s threshold value for tree transpiration was estimated, on the basis of the fact that Yatir forest is dominated by *P. halepensis*, a tree species exhibiting nearly complete

stomatal closure at leaf water potential (Ψ_l) around -2·8 MPa (Klein *et al.*, 2011). To allow the ascent of water up the tree and along the soil–plant–atmosphere continuum, a water potential difference between soil and leaf must prevail. In plant canopies where Ψ_s is highly variable, as in Yatir, this water potential gradient may fluctuate between 0·5 and 1·1 MPa (Elfving *et al.*, 1972; Jones and Turner 1978). It is by using an average soil–leaf water potential gradient of 0·8 MPa that a Ψ_s value of $-2{\cdot}0$ MPa is expected to induce nearly complete stomatal closure and hence a strong reduction in root water uptake.

Root depth distribution

During a forest-scale soil survey in September 2011, 22 trenches, 1- to 1·8-m deep and 5- to 7-m long, were dug in Yatir forest. In each trench, three vertical profiles were chosen, at about 0·1–1 m from tree trunk bases. Root diameter was measured using a digital calliper (indication error 0·03 mm; Fuji, Japan) for all roots larger than 0·5 mm diameter and captured within a 20 cm × 20 cm frame that was placed onto the trench's wall in consecutive soil depths ($N = 5$–9). Root density (roots m^{-2} of soil surface) was then calculated for five different root diameter classes. Soil depth and stone fraction were also measured and recorded.

Tree water use

Between September 2009 and March 2010, sap flow sensors were installed on 16 trees in Yatir forest, at about 70 m from the flux tower. Lab-manufactured thermal dissipation sensors (Granier and Loustau 1994) were applied to all trees, and commercial heat balance sensors (EMS, Brno, Czech Republic; Cermak *et al.*, 2004) were also used on six of these trees. Measurements were taken every 30 s, and the 30-min average was saved on a local CR1000 data-logger (Campbell Scientific Inc., Utah, USA) and transmitted via internet to the lab at the Weizmann Institute of Science. Sap flow rates (SF, kg h^{-1} $tree^{-1}$) were calculated in relation to the minimum sap flux during a 24-h period, as shown in the empirical equation of Granier and Loustau (1994), modified by Kaneti (2010):

$$\mathrm{SF} = \mathrm{LCF} \times \mathrm{CF} \times 0{\cdot}04284 \times [(\Delta T_{\max} - \Delta T_r)/\Delta T_r]^{1.231} \quad (2)$$

where LCF is the length compensation factor due to the inability of the 2-cm probes to capture the entire active sapwood depth, but rather 65% of it (for *P. halepensis* in Yatir; Cohen *et al.*, 2008) and calculated for each individual tree; CF is a calibration factor of 2·5 (Kaneti, 2010; Steppe *et al.*, 2010); ΔT_r is the average half-hourly temperature difference between heated and non-heated probes; and $\Delta T_{\max}$ is the maximum temperature difference measured over the 24-h period. The calibrated SF values correlated well with SF measurements using the heat balance method ($r^2 = 0{\cdot}90$, regression slope of 0·82). The radial gradient of sap velocity in these trees was quantified in an earlier study (Cohen *et al.*, 2008), indicating a quasi-linear decrease from maximum sap velocity at 5 mm below the cambium down to zero at 40 mm. Diurnal totals were further calculated and transformed into sap flux densities, according to

$$\mathrm{SFD} = \sum(SF)/A_{sw} \times 1000 \quad (3)$$

where SFD is the diurnal sap flux density (cm^3 d^{-1} cm^{-2}) and A_{sw} is the sapwood area of each individual tree. The summation in Equation (3) is applied to all measured data points within a day. Tree transpiration (T_t, mm d^{-1}) was calculated as the mean sap flux density of all trees multiplied by stand density (300 trees ha^{-1}) and the mean sapwood area of 216 cm^2. T_t was identified as one of four components of total ET:

$$ET = T_t + T_u + I + E_s \quad (4)$$

where T_t is tree transpiration, T_u is transpiration from understory vegetation (usually confined to the rainy season), I is evaporation of water intercepted by plant foliage, and E_s is evaporation from soil. The understory vegetation is dominated by the bush species *Sarcopoterium spinosum* and *Retama raetam*, accompanied by annuals and geophytes (e.g. *Ophrys umbilicata* and *Tulipa systola*), and its total biomass reaches 0·3–1 kg DW m^{-2} during the wet season.

$\delta^{18}O$ in water from soil and tree sap

Soil water was extracted from samples at depths of 0, 5, 10, 20, 30 and 40 cm taken on four field days: 13 September 2004 (summer), 16 December 2004 (autumn), 6 January 2005 (winter) and 14 March 2005 (spring). A fresh core was dug each field day from a small, defined area within the flux tower plot, to maintain constant soil characteristics while sampling an uninterrupted profile. During each field day, sap water was also collected from two chosen trees. Samples from each depth or tree were stored in glass containers, sealed and refrigerated until analysed. At the laboratory, water was removed from the samples by distillation in a vacuum line (Wang and Yakir 2000), sealed and kept refrigerated until analysed for isotopic composition of $\delta^{18}O$ using isotope ratio mass-spectrometry, as described in the study of Barrie and Prosser (1996). To partition the proportional contribution of each soil depth water source to sap water, measurements were statistically analysed with the mixing model IsoSource (Phillips and Gregg 2003), providing the distribution of feasible isotopic mass balance solutions. The source increment was set at 1%, and the mass balance tolerance at 0·1.

Simulation of soil water content dynamics

Soil water content was simulated using the multilayer, multi-leaf process-based biosphere–atmosphere gas exchange model MuSICA (Ogee *et al.*, 2003). This model is optimally suited for studies on coniferous forests because it explicitly accounts for needle clumping of various needle cohorts and was successfully tested and used in such studies (e.g. Ogee *et al.*, 2003; Ogee *et al.*, 2009). The model allows the computation of scalar vertical profiles (e.g. air temperature and CO_2) and the different component fluxes of the carbon, water and energy budget. Notably, it gives separate estimates of not only tree water use (T_t), gross primary productivity and

net ecosystem exchange (NEE) but also soil moisture profile for each modelled soil layer. The version 2.0.x used in this study has been upgraded compared with the versions 1.x.x used in previous publications (e.g. Ogee *et al.*, 2003; Ogee *et al.*, 2009). MuSICA parameters, such as profiles of soil porosity, soil matric potential and soil hydraulic conductivity at saturation (Table I), as well as rooting profile (Table II), were taken from aforementioned site-specific managements. Photosynthesis and phenological parameters were taken from previously published measurements (Maseyk *et al.*, 2008).

RESULTS

Soil water content dynamics and mechanical structure

Measurements in the soil were divided into four depth layers: 0–10, 10–20, 20–40 and 40–60 cm (layers I–IV). Mean values for the 5-year study period indicated that in summer SWC strongly increased with depth, ranging from 7% in layer I to 21% in layer IV [Figure 1(a)]. In autumn, just before the start of the rainy season, all layers were even dryer, except for layer I, where occasionally 1–2 early rain events elevated SWC up to 11%. The sharp gradient expired in winter, when SWC was 18–20% along the entire soil profile. In spring, soil had already started to dry out, except in layer IV, where an average SWC of 18–20% prevailed all year round.

Mechanical soil properties were likely to play an important role in these seasonal dynamics. Generally, there was an increase in clay content and a decrease in sand content with depth, particularly in the transition between layers III and IV [Figure 1(b)]. Layer IV was different from the other layers in its mechanical composition, with less than 5% sand and more than 50% clay. The finer soil texture (and increased water retention capacity) in layer IV is associated with the maintenance of SWC above 18% all year round. Higher sand content (up to 51%) and lower clay content (down to 32%) were found in shallower layers, indicating a coarser soil texture closer to the surface.

Table I. Soil parameters of van Genuchten–Mualem model Equation (1) for Yatir soil, obtained by RETC software.

Soil layer	Depth (cm)	θ_r	θ_s	α	n	m
I	0–10	0·0754	0·4009	0·0245	1·2910	0·2254
II	10–20	0·0834	0·4201	0·0244	1·2579	0·2050
III	20–40	0·0867	0·4283	0·0262	1·2281	0·1857
IV	40–60	0·1050	0·5138	0·0150	1·3102	0·2368

Retention curves in Figure 2 are the parameters' respective graphic solutions of Equation (1) for discrete depths.

Soil water retention properties

On the basis of their mechanical structure, layer-specific van Genuchten–Mualem soil parameters were calculated using the RETC software (Table I), and water retention curves were plotted [Figure (2)]. The exponential nature of all curves demonstrated that for SWC above 20%, soil water potential (Ψ_s) was high and stable (between -0·1 and -0·6 MPa depending on the layer), whereas at low SWC values minor shifts in SWC meant major water potential changes. Applying the soil water retention curves to the layer-specific SWC measurements in a given year [Figure 3 (a)] produced layer-specific Ψ_s curves for that year [Figure 3(b)]. Errors associated with the SWC data and the retention curve estimation were propagated in this calculation according to error propagation rules (Taylor 1997) and reported in Figure 3. Applying the Ψ_s threshold for T_t ($-2{\cdot}0$ MPa, see Materials and Methods section) to the layer-specific retention curves (Figure 2), we then estimated SWC thresholds for T_t (ttSWC). We obtained values of $13{\cdot}2 \pm 0{\cdot}3\%$, $15{\cdot}2 \pm 0{\cdot}4\%$, $17{\cdot}0 \pm 0{\cdot}7\%$ and $17{\cdot}6 \pm 0\%$ for layers I–IV, respectively. The strong increase in these thresholds with soil depth emphasizes the importance of taking into account depth-resolved soil properties. Because the ttSWC value for layer IV (17·6%) was lower than the corresponding 5-year minimum SWC value (18·9%), unlike in other layers, we chose to use the observed minimum value as a more reliable estimate of ttSWC for layer IV, although this did not have a large impact on our results.

Transpirable soil water content and tree water use

Once the ttSWC thresholds estimated for each soil layer, we defined and calculated transpirable soil water content (tSWC, mm) as follows:

$$\mathrm{tSWC} = h \times (1 - \mathrm{ST}) \times (\mathrm{SWC} - \mathrm{ttSWC}) \qquad (5)$$

Table II. Mean (SE) number of roots per square metre of trenched depth profile as function of soil depth, divided into five root diameter categories ($n = 22$ trenches).

Soil layer	Depth (cm)	0·5–2	2–5	5–10	10–20	>20 mm
I + II	0–20	317 (37)	165 (21)	74 (11)	42 (9)	9 (3)
III	20–40	334 (34)	160 (17)	52 (8)	25 (7)	8 (3)
IV	40–60	241 (32)	70 (16)	24 (5)	6 (3)	1 (1)
V	60–80	126 (21)	50 (18)	8 (3)	3 (2)	1 (1)
VI	80–100	32 (7)	7 (2)	1 (1)	1 (1)	0 (0)
VI	100–120	27 (9)	3 (2)	0 (0)	1 (1)	0 (0)
VI	120–140	7 (4)	0 (0)	1 (1)	0 (0)	0 (0)
VI	140–160	1 (1)	1 (1)	0 (0)	0 (0)	0 (0)
VI	160–180	0 (0)	0 (0)	0 (0)	0 (0)	0 (0)

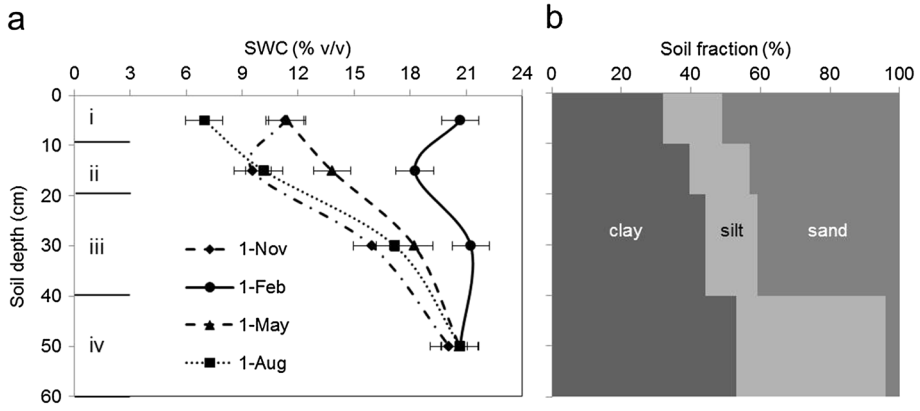

Figure 1. Five-year (2006–2009) seasonal soil water content (SWC) changes ($n = 5$, *means* ± *SE*) in four depth layers (labelled I–IV) in Yatir forest (a) and their mechanical composition (b). Note that both SWC dynamics and sand/clay ratio decrease with depth.

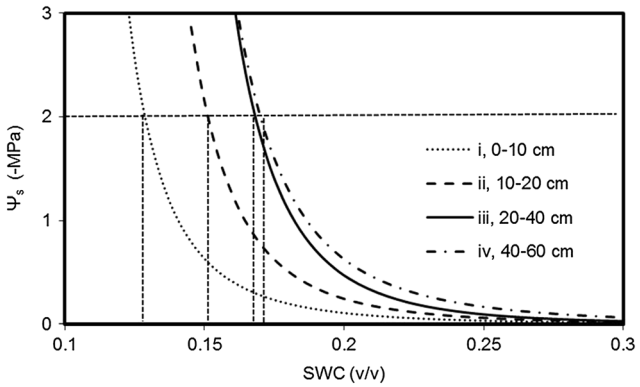

Figure 2. Soil water retention curves for four depth layers in Yatir forest (based on Equation (1) and Table I). Horizontal dash line denotes the soil water potential (Ψ_s) threshold value for *Pinus halepensis* transpiration (when $T_t = 0$). The corresponding soil water content (SWC) values were 13·2 ± 0·3, 15·2 ± 0·4, 17·0 ± 0·7 and 17·6 ± 0% for layers I–IV, respectively. The shape of the retention curves demonstrates an increasing sensitivity to small changes in SWC as the Ψ_s threshold is approached.

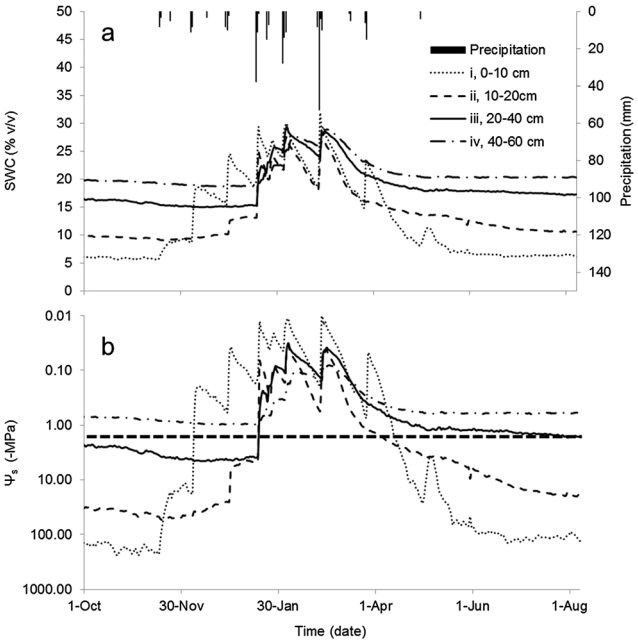

Figure 3. Seasonal dynamics in precipitation and soil water content ((a), SWC, $n = 2$–3 pits) and soil water potential ((b), Ψ_s, logarithmic scale; calculated using Equation (1) and Table I) in four depth layers in Yatir forest during the 2010 growth season. Horizontal dash line in (b) denotes the soil water potential threshold value for *Pinus halepensis* transpiration (when $T_t = 0$). *SEs* for SWC measurements (Materials and Methods) are 0·1–1·6, 0·4–4·2, 0·0–4·8 and 0–4·7% v/v for layers I–IV, respectively. Propagated *SEs* for calculated Ψ_s are 0·03–0·29, 0·08–0·65, 0·05–0·53 and 0–0·45 MPa for layers I–IV, respectively.

and for the entire soil profile,

$$\sum_{\text{i-vi}} \text{tSWC} = \sum h \times (1 - \text{ST}) \times (\text{SWC} - \text{ttSWC}) \quad (6)$$

where h is the height of the soil layer (mm) and ST is its stone fraction, and the summation is performed over six soil layers (layers I–IV and two deeper layers complementing for the entire soil profile in this site). This term develops the existing terms for water availability, which are discussed in the Introduction, by providing absolute quantity rather than a fraction, which can be directly used in hydrological budgets. In addition, we link this term to species-specific root water uptake threshold and to depth-dependent soil characteristics. SWC data in each layer over the 5-year study period were then transformed into tSWC using Equation (5). Errors in tSWC were calculated according to error propagation rules (Taylor 1997) and reported in Figure 4. Focusing on 2010, as a representative year with the most complete measurement sets, we found that soil water availability was highly influenced by precipitation patterns as shown in an annual tSWC diagram [Figure 4(a)]. In particular, tSWC peaked in all layers following the first rain storm in 17–19 January ($P = 50$ mm), marking the onset of the wet season, and diminished (in layers III and IV) or vanished altogether (in layers I and II) 2 weeks after the last significant rain event on 28 March, marking the onset of the drying season. Layer I also responded to the light rains marking the onset of the wetting season (17–18 November, $P = 11$ mm), despite the absence of deeper infiltration. Finally, layer II had the lowest positive values of tSWC and the shortest period. Considering the water retention properties and spatial situation of this layer, this was mainly the result of rainwater infiltration into deeper layers, as layers III and IV maintained positive tSWC values throughout the summer drought.

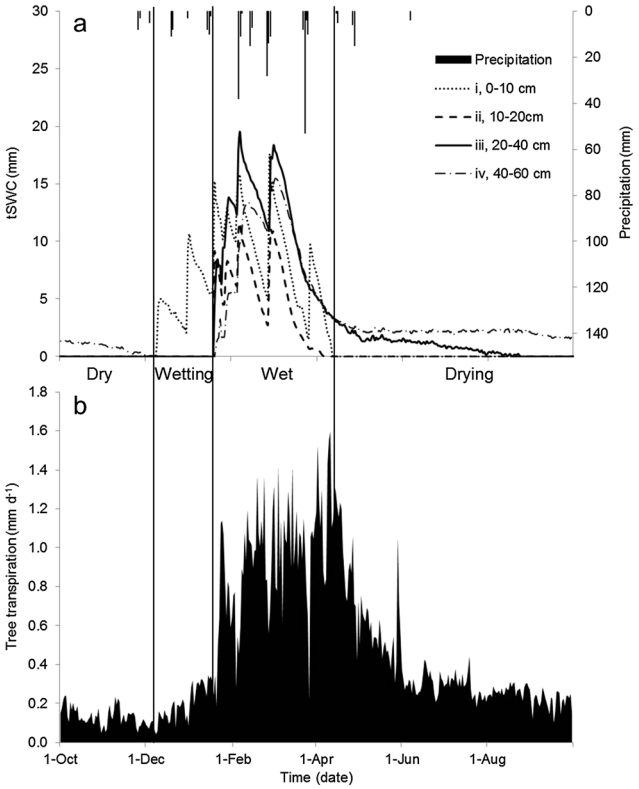

Figure 4. Seasonal dynamics in precipitation and transpirable SWC (tSWC, $n = 2$–3 pits) in four depth layers (a), and in tree transpiration (T_t, measured in up to 16 trees, b) in Yatir forest during the 2010 growth season. The increase in T_t during the wetting period relied on layer I; Persisted T_t throughout the dry season relied on tSWC below 20 cm. Propagated *SEs* for tSWC calculations (Materials and Methods) are 0·12–0·42, 0·07–0·38, 0·50–1·05 and 0·53–0·96 mm for layers I–IV, respectively.

The tSWC diagram was further compared with continuous, parallel measurements of tree transpiration [Figure 4 (b)]. During the dry period, prior to the emergence of soil water availability in layer I on 8 December, very low T_t levels (0·1–0·2 mm d^{-1}) prevailed, partly explained by a residual tSWC in layer IV. At the wetting period (prior to 18 January), low T_t levels (0·2–0·4 mm d^{-1}) were supported by layer I. After that date, high T_t levels (up to 1·6 mm d^{-1}) were observed, corresponding to positive tSWC values in all four soil layers. Non-zero T_t values after 14 April, when no soil water remained available above 20 cm, indicated a high reliance of T_t on soil water from layers III and IV. Additional water amounts were also available in deeper layers but with smaller contribution to T_t (see next section). Above-ground conditions also affected tree transpiration. In particular, the T_t peak in late spring is explained by an optimal combination of water vapour pressure deficit, solar radiation, temperature and plant phenology (Maseyk *et al.*, 2008). However, once no soil water remained available above 20 cm, rapid decline in T_t was imposed irrespective of the other factors.

Annual soil water budget is influenced by depth-dependent infiltration

The depth-dependent change in soil water retention discussed previously clearly influenced the water distribution in the soil profile and its dynamics. Layer-specific infiltration water amounts (mm) were determined using the calculation of layer-specific diurnal SWC change (dSWC, mm), as adapted from Li *et al.* (2002):

$$\mathrm{dSWC} = h \times (1 - \mathrm{ST}) \times (\mathrm{SWC_d} - \mathrm{SWC_{d\text{-}1}}) \quad (7)$$

where $\mathrm{SWC_d}$ and $\mathrm{SWC_{d-1}}$ are the SWC values of the current and previous day, respectively. Typically to semi-arid environments, SWC fluctuations were larger in shallow layers than in deeper layers [Figure 3(a)]. In a typical precipitation event on 17–19 January with a total amount of 50 mm, we calculated that 10, 11, 12 and 2 mm of water infiltrated into layers I–IV, respectively, and none to deeper layers, meaning that 70% of the water input reached the upper 40 cm of the forest soil and 30% was lost through evaporation from the soil, litter and leaf surfaces. The 2010 annual water budget followed an analogous partitioning: we calculated that out of 289 mm of rain, 228 mm infiltrated into the soil, and the residual 61 mm was lost in interception and soil surface evaporation. Using Equation (6), we estimated that out of the infiltrated 228 mm, as much as 202 mm was available for transpiration (tSWC) and was partitioned into six soil layers (Figure 5). Ultimately, sap flow data indicated that of the tSWC, trees actually used 164 mm, and the residual 38 mm presumably partitioned into transpiration from understory vegetation (Equation (4)).

Root depth distribution

Root distribution across the soil profile supported the idea that T_t highly relied on tSWC in the 20- to 40-cm soil layer. Measurements of root distribution indicated a nearly linear decline with depth from the soil surface down to 1 m, and only very few roots were identified below that level (Table II). The number of fine roots (<2 mm) in layer III was, however, slightly higher than in layers I and II. Although a few fine roots were occasionally found below 1 m, the majority of the rhizosphere was confined to higher layers: 66% of roots were above 40 cm (layers I–III) and 85% above 60 cm (layers I–IV).

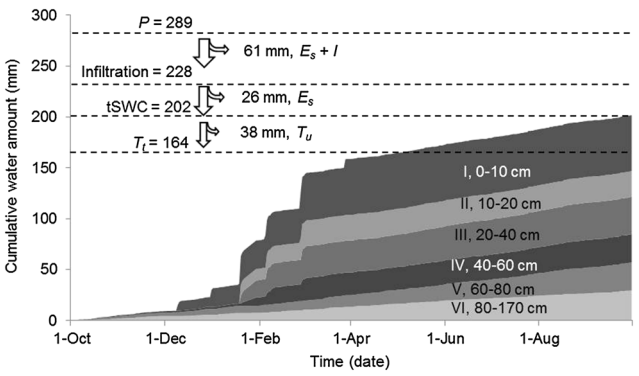

Figure 5. Partitioning of precipitation water (P) to hydrological components at Yatir forest during the 2010 growth season (dash lines) and the accumulation over time of transpirable SWC (tSWC, $n = 2$–3 pits) in the different soil layers. E_s, evaporation from soil; I, evaporation of water intercepted by plant foliage; and T_u, transpiration from understory vegetation.

Water $\delta^{18}O$ of soil and tree sap

Comparing the oxygen isotope composition of soil water from different depths with that of xylem water (not exposed to evaporation) can provide an indicator of the depth of water uptake, if vertical variations in oxygen isotope composition of soil water through the rooting zone are sufficiently large (Zimmermann *et al*., 1966; Walker and Brunel 1990; Wang and Yakir 2000). However, sap water $\delta^{18}O$ usually reflects a complex mixture of water from multiple depths, and hence, a statistical approach is needed (Phillips and Gregg 2003). Results from the IsoSource mixing model applied to our $\delta^{18}O$ data indicated a seasonal shift in depth of water use over the season (Table III). Specifically, the summer $\delta^{18}O$ values seem to indicate a significant contribution from layer III (~70% in average). In autumn, layer II was identified as the primary water source, whereas in winter, the water source seemed equally partitioned among layers I–III (but with large uncertainty due to homogeneity of the soil water $\delta^{18}O$ profile). Finally, in spring, layer III was identified by the isotope mixing model as the primary water source (~80% in average).

Relationship between soil texture and water content from ecosystem model simulations

To study the relationship between soil texture and water content, we used the ecosystem gas exchange model MuSICA (Ogee *et al*., 2003). The SWC in layer III was simulated in two different scenarios: (1) using the more conventional approach of bulk hydraulic properties, applying layer II properties on the entire profile; and (2) using the observed layer-specific soil hydraulic properties as in Table I. Results from the two simulations show that the bulk approach of scenario (1) yielded relatively low soil moisture during the dry season, reflecting unsustainable forest water balance, whereas the more realistic scenario (2) captured the observed, higher SWC during the dry season (Figure 6). Moreover, the difference between the two simulations is emphasized considering their opposite relation to the tSWC threshold of 17%: tSWC is maintained in the root zone in scenario (2) but clearly not in (1).

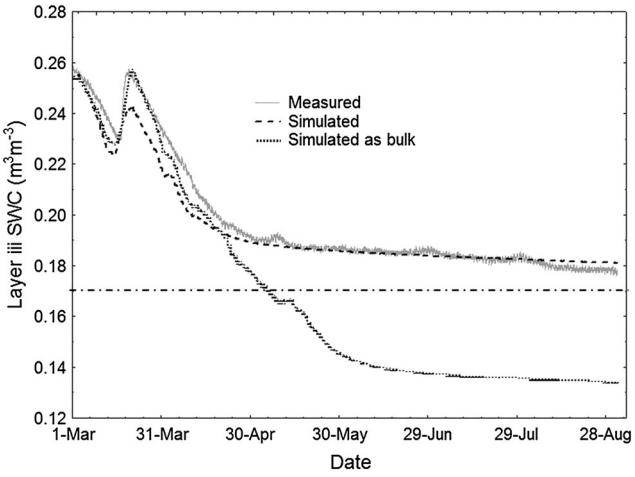

Figure 6. Soil water content (SWC, $n = 3$) dynamics in layer III measured in Yatir forest during 2007 and simulated with MuSICA in two scenarios: (1) using layer II soil hydraulic properties for the entire profile (simulated as bulk), and (2) using observed layer-specific soil hydraulic properties as in Table I (simulated). Using the more conventional approach of bulk hydraulic properties (scenario 1) resulted with lower soil moisture during the dry season, below the tSWC threshold (horizontal line), and creating an unsustainable forest ecosystem.

DISCUSSION

Depth-dependent water availability

Our results indicate that for 2010, the total T_t and P values in Yatir forest were 164 and 289 mm, respectively, yielding a T_t/P ratio of 0·57. This ratio is consistent with a previous estimate of 0·53 for the same forest (Raz-Yaseef *et al*., 2010a) but notably higher than values reported for other conifer forests (0·1–0·5; Roberts 1983) and also for different semi-arid ecosystems (0·35; Miller 1982; Paruelo *et al*., 2000). Considering only the water that infiltrated into the soil (228 mm, Figure 5) yields even higher ratio of 0·72, indicating only little losses to recharge and soil evaporation, with most of the infiltrating water available for transpiration. We suppose that this high ratio is also strongly linked to depth-dependent soil properties. It was shown in previous forest ecohydrology studies that variability of soil texture with depth affected Ψ_s (Breda *et al*., 1995; Warren *et al*., 2005). Specifically, high (45%) clay content layers were associated with more negative Ψ_s values (for a given SWC) and lower rooting density (Breda *et al*., 1995).

Here, we show that the high availability of water for transpiration is also supported by local soil structure, composed of a water holding layer III lying on top of a high retention layer IV. The relatively coarse layer III [sand fraction >40%, Figure 1(b)] was a major water source for T_t (Figures 4 and 5) and was acting as a buffer by allowing a suspended release of rainfall water across weeks and

Table III. Partitioning of water sources for tree transpiration using a stable isotope mixing model (Phillips and Gregg 2003).

Soil layer	Depth (cm)	Summer	Autumn	Winter	Spring
I	0	5·6 (5·0)	1·4 (1·5)	7·8 (5·2)	0·1 (0·3)
I	5	10·2 (8·7)	1·9 (1·9)	7·2 (4·8)	2·8 (2·7)
I	10	7·3 (6·3)	4·3 (3·9)	26·4 (20·6)	4·8 (4·4)
II	20	6·1 (5·4)	90·5 (3·1)	29·3 (19·9)	2·4 (2·4)
III	30	14·8 (12·5)	1·9 (1·9)	29·3 (19·9)	8·0 (7·1)
III	40	56·1 (7·0)	n.a.	n.a.	82·0 (6·2)

Mean percent (SD) for distributions of feasible solutions of water $\delta^{18}O$ isotopic mass balance, on the basis of tree sap as mixture and soil water as sources.

months. Water availability is maintained in this layer for months after the rainy season [unlike in shallower layers, Figure 4(a)], and its stone fraction of 21% is lower than that of deeper layers (e.g. 48% at 90 cm and up to 100% at 170 cm). In contrast to layer III, high clay content (>50%) in layer IV [Figure 1(b)] means that its baseline SWC of ~20% is essentially non-transpirable, but it minimizes infiltration and losses into deeper soil layers, thus allowing the accumulation of water in the soil above it. Evidence for such accumulation comes from SWC values exceeding field capacity in layers I and III but not in other layers. For example, at 25 cm depth, we measured SWC values of up to 31%, whereas field capacity value (SWC at −0·033 MPa; Israelson and West 1922) was calculated as 30% (in contrast, at 50 cm depth, maximum SWC was 33%, still below the field capacity value of 35%). Additional evidence is provided by model simulations, where prolonged water availability in layer III is associated with the limited infiltration to depths below 40 cm and into the high water retention layer (Figure 6).

The role of layers I and II in the tree water use is important during the rainy season, with both hydraulic (Figure 4) and isotopic (Table III) evidence.

In an ecosystem already restricted by soil depth (33–124 cm, data not shown), the rhizosphere is furthermore concentrated in the 0- to 60-cm layers (Table II). This narrow root distribution can be explained by changes in the transpirable water content of the various depth layers: fine root density peaks in layer III and declines in the high retention layers below it. Dependence of vertical root distribution in water availability was shown in an oak stand (Breda *et al*., 1995), and also in *P. halepensis* and the closely related *Pinus brutia* (Querejeta *et al*., 2001; Ganatsas and Tsakaldimi 2003, respectively). A similar, narrow root distribution was described in a *P. brutia* forest grown on shallow, stony soil in Greece (Ganatsas and Tsakaldimi 2003). Yet, in a deep soil site (average soil depth ~100 cm), *P. halepensis* roots were concentrated between 80 and 100 cm, and none above 40 cm (van Beek *et al*., 2005). Note, however, that the correlation between water use and root distribution can be nonlinear: a few sinker roots may dominate tree water uptake (Mickovski and Ennos 2003) especially under stress (Nadezhdina *et al*., 2007), and the correlation can be complicated by hydraulic redistribution, i.e. root-assisted vertical water transport (Nadezhdina *et al*., 2006).

Inter-annual variations in transpirable soil water content

On the inter-annual time scale, one of the important issues to consider is defining the growth season (i.e. delineating its onset and termination). In water-limited ecosystems such as the study site, tree growth highly coincides with water availability (Klein *et al*., 2005; Maseyk *et al*., 2008; Klein *et al*., 2012), and we therefore propose to define the growth season using tSWC estimates. Predictions of the onset of the growth season have so far mostly relied on precipitation data, with obvious difficulties in characterizing rainfall events by their intensity (e.g. mm d^{-1}) or their frequency of occurrence (i.e. effective time between two events; e.g. in Zeppel *et al*., 2008; Raz-Yaseef *et al*., 2012). Figure 4 shows that emergence of tSWC in layers II–IV on 18 January (vertical line marking the onset of the wet season) was shortly followed by a threefold increase in transpiration rates starting from 21 January, potentially marking the onset of the growth season in winter (Maseyk *et al*., 2008). Further coordinated sap flow and SWC measurements should improve the predictability of the onset of growth season.

However, it is probably more important to examine the association between tSWC and the termination of the growth season, which can greatly influence forest sustainability and actual survival. Inter-annual variations in tSWC reflected variations in total annual precipitation as well as in the timing of the first and last rain events [Figure 7(a)]. It is the time between the last rain of a given growth year and the first rain of the following growth year that defines the length of the drought interval. During the dry season, T_t relied mainly on layer III (Figure 4) and to a lesser extent, on deeper layers. Therefore, maintaining T_t across the drought period depends on the water dynamics in this layer, which varied between years [Figure 7(a)]. For example, in summer 2006, trees had a continuous water supply (indicated by positive tSWC values in layer III across the entire length of the dry season). In contrast, in 2007, transpirable water was unavailable for nearly 2 months before the onset of the next active season on 20 December [Figure 7(a)]. Even longer water shortages were observed in the summer seasons of 2008 and 2009, lasting about 5 and 4 months, respectively.

Notably, during the consecutive drought years of 2008 and 2009, interruptions in tSWC in layer III are correlated with increase in observed tree mortality, affecting 5–10% of the trees in Yatir. The ability of *Pinus halepensis* to survive intense and prolonged drought has been shown in the field (Maseyk *et al*., 2008; Schiller and Atzmon 2009). In a controlled drought experiment, *P. halepensis* saplings exposed to 3-week drought cycles demonstrated a 90% survival rate, even at only 25% of the optimal water supply (Klein *et al*., 2011). Being a drought-avoiding species, *P. halepensis* may enforce stomatal closure for periods longer than a month, risking negative carbon balance and carbon starvation, potentially leading to mortality. Our results indicate that the difference between survival and large-scale tree mortality may be related to the length of period with positive tSWC. In the study period, this was reflected in the difference between 2 and 4 months of zero tSWC in 2007 versus 2009 [Figure 7(a)]. On the basis of our preliminary 5-year study, we propose a threshold value of about 3 months zero tSWC for *P. halepensis* forest sustainability at our site.

Could the date of tSWC exhaustion be estimated? It seems that this is possible at least on a seasonal basis. A careful examination of the inter-annual patterns of tSWC in layer III [Figure 7(b)] suggests that although the spans of soil moisture availability varied between years, tSWC quenching rate followed a similar pattern. Linear regressions of layer III tSWC decline between 30 April (which

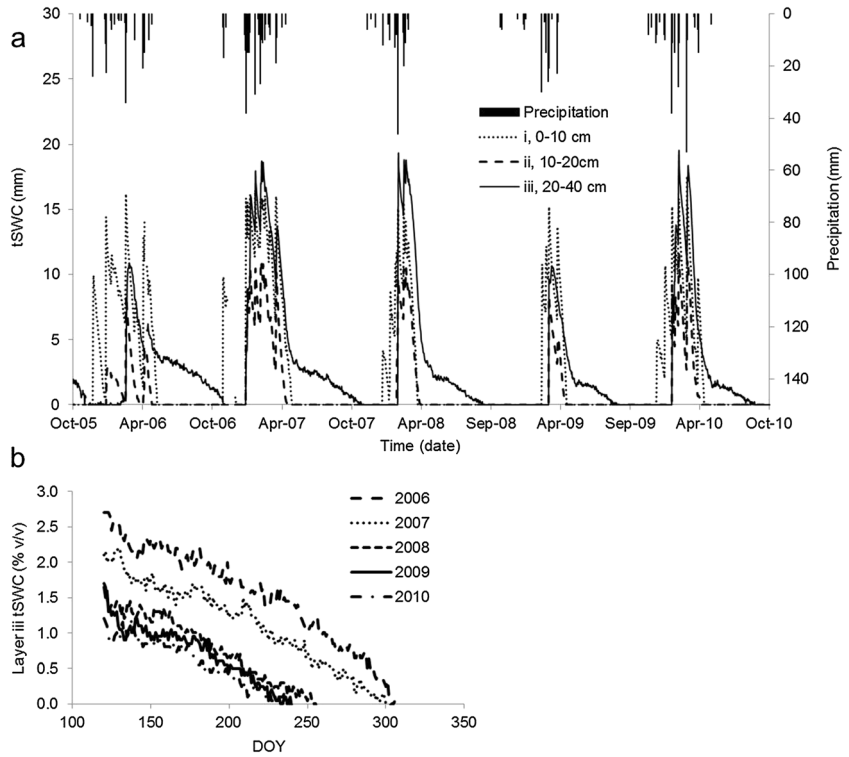

Figure 7. (a) Transpirable soil water content (tSWC, $n = 2$–3) in three depth layers and precipitation in Yatir forest during 2006–2010 (annual precipitation amounts were 224, 308, 200, 160 and 289 mm, respectively). Droughts during 2008 and 2009 resulted in long intervals (up to 5 months) of zero water availability, ultimately leading to large-scale tree mortality. (b) Zooming in on the linear decline of tSWC in layer III after 30 April. Regression slopes are -0·012, -0·011, -0·012, -0·011 and -0·009% d^{-1} for 2006–2010, respectively ($R^2 = 0{\cdot}92$–$0{\cdot}97$), allowing early estimate of the date of tSWC exhaustion in this forest ecosystem.

was always after the last significant rain event) and the last date of water availability on time, generated slopes of -0·012, -0·011, -0·012, -0·011 and -0·009% d^{-1} for 2006–2010, respectively ($R^2 = 0{\cdot}92$–$0{\cdot}97$). Therefore, the last date of positive tSWC in layer III (and the layers above it) for a given year can be estimated according to

$$t_f = t_i + (\mathrm{tSWC_{ti}}/0{\cdot}011) \quad (8)$$

where t_f is the final date of water availability, t_i is the initial date of linear quenching (30 April) and $\mathrm{tSWC_{ti}}$ is the initial layer III tSWC on 30 April. Also, this means that a last date of water availability can be predicted by the end of April, still before summer. For example, using Equation (7), an initial layer III tSWC of 3% should suffice up to 30 September. Together with the aforementioned 3-month drought threshold, this means that in such scenario, significant precipitation must come before 30 December to ensure forest sustainability. The ability to clearly define the timing of tSWC exhaustion has implications for estimating the growth season length, and forest productivity and sustainability under different climate change (precipitation) scenarios.

CONCLUSIONS

Amounts of transpirable soil water (tSWC) are readily calculated from SWC measurements and soil water retention data. These tSWC estimates were shown to explain tree water use and its seasonal changes, thereby providing an effective approach to assess the ecohydrology of forest ecosystems. On the basis of this approach, we further concluded that the success of the water-limited pine forest relied on high T_t/P (0·57) that reflected, in turn, the existence of high retention layer below the root zone. These results greatly improved model simulations of the forest ecohydrology that otherwise showed an unsustainable nature of the ecosystem.

ACKNOWLEDGEMENTS

This work was supported by KKL-JNF (Alberta-Israel program 90-9-608-08), Sussman Center, Cathy Wills and Robert Lewis Program in Environmental Science, France-Israel High Council for Research Scientific and Technological Cooperation (project 3-6735), and the Minerva Foundation. T. K. acknowledges the Karshon foundation and the Rieger foundation grants. T. K. thanks Dr Jiri Kucera of EMS Ltd., Czech Republic, and Prof. Katarina Strelcova of Zvolen technical university, Slovakia, for training with the sap flow measurement system. T. K. thanks Tal Kaneti of ARO Volcani, Israel, for assistance in sap flow sensor manufacturing. E. C. H. thanks Dr Guy Levi of ARO Volcani and Tsila Aviad of the Hebrew University of Jerusalem for providing experimental equipment for soil analysis. Helpful comments on a previous version of the manuscript were provided by two anonymous reviewers.

REFERENCES

Barrie A, Prosser SJ. 1996. *Automated Analysis of Light-element Stable Isotopes by Isotope Ratio Mass Spectrometry, Mass Spectrometry of Soils*, Boutton TW, Yamasaki S (eds). Marcel Dekker Inc.: New York. 1–46.

Bond BJ, Kavanagh KL. 1999. Stomatal behavior of four woody species in relation to leaf-specific hydraulic conductance and threshold water potential. *Tree Physiology* **19**: 503–510.

Bouyoucos GS. 1962. Hydrometer method improved for making particle size analysis of soils. *Agronomy Journal*, **54**: 464–465.

Breda N, Granier A, Barataud F, Moyne C. 1995. Soil water dynamics in an oak stand. *Plant and Soil* **172**: 17–27.

Cermak J, Kucera J, Nadezhdina N. 2004. Sap flow measurements with some thermodynamic methods, flow integration within trees and scaling up from sample trees to entire forest stands. *Trees* **18**: 529–46.

Christensen JH, Hewitson B, Busuioc A, Chen A, Gao X, Held I, Jones R, Kolli RK, Kwon W-T, Laprise R, Magaña Rueda V, Mearns L, Menéndez CG, Räisänen J, Rinke A, Sarr A, Whetton P. 2007. Regional climate projections. In *Climate Change 2007: The Physical Science Basis. Contributions of Working Group I to the Fourth Assessment Report of the Intergovernmental Panel on Climate Change*, Solomon S, Qin D, Manning M, Chen Z, Marquis M, Averyt KB, Tingor M, Miller HL (eds). Cambridge University Press: Cambridge, United Kingdom/New York, NY.

Cohen Y, Cohen S, Cantuarias-Aviles T, Schiller G. 2008. Variations in the radial gradient of sap velocity in trunks of forest and fruit trees. *Plant and Soil* **305**: 49–59.

Domec JC, King JS, Noormets A, Treasure E, Gavazzi MJ, Sun G, McNulty SG. 2010. Hydraulic redistribution of soil water by roots affects whole-stand evapotranspiration and net ecosystem carbon exchange. *New Phytologist* **187**: 171–183.

Elfving DC, Kaufmann MR, Hall AE. 1972. Interpreting leaf water potential measurements with a model of the soil-plant-atmosphere continuum. *Physiologia Plantarum* **27**: 161–68.

Ganatsas PP, Tsakaldimi MN. 2003. Root system modification of *Pinus brutia* Ten. Species under adverse ecological conditions. 8th International Conference on Environmental Science and Technology, Lemnos Island, Greece, 8-10 Sep 2003.

Gollan T, Turner NC, Schulze ED. 1985. The responses of stomata and leaf gas exchange to vapour pressure deficits and soil water content III. In the sclerophllous woody species *Nerium oleander*. *Oecologia* **65**: 356–62.

Granier A, Loustau D. 1994. Measuring and modeling the transpiration of a maritime pine canopy from sap-flow data. *Agricultural and Forest Meteorology* **71**: 61–81.

Granier A, Breda N, Biron P, Villette S. 1999. A lumped water balance model to evaluate duration and intensity of drought constraints in forest stands. *Ecological Modeling* **116**: 269–83.

Gruenzweig JM, Lin T, Rotenberg E, Schwartz A, Yakir D. 2003. Carbon sequestration in arid land forest. *Global Change Biology* **9**: 791–799.

Gruenzweig JM, Gelfand I, Yakir D. 2007. Biogeochemical factors contributing to enhanced carbon storage following afforestation of a semi-arid shrubland. *Biogeosciences* **4**: 891–904.

Gupta SC, Larson WE. 1979. Estimating soil water retention characteristics from particle size distribution, organic matter percent, and bulk density. *Water Resources Research* **15**: 1633–5.

Heiskanen J, Makitalo K. 2002. Soil water retention characteristics of Scots pine and Norway spruce forest sites in Finnish Lapland. *Forest Ecology and Management* **162**: 137–152.

Israelson OW, West FL. 1922. Water holding capacity of irrigated soils. *Utah State Agricultural Bulletin* **183**: 1–24.

Jones MM, Turner NC. 1978. Osmotic adjustments in leaves of Sorghum in response to water deficits. *Plant Physiology* **61**: 122–6.

Kaneti T. 2010. Yield and physiological and environmental stress indices in persimmon trees irrigated with various grades of treated water. Thesis, The Hebrew University of Jerusalem, Rehovot, Israel.

Klein T, Hemming D, Lin T, Grünzweig JM, Maseyk KS, Rotenberg E, Yakir D. 2005. Association between tree-ring and needle delta C-13 and leaf gas exchange in *Pinus halepensis* under semi-arid conditions. *Oecologia* **144**: 45–54.

Klein T, Cohen S, Yakir D. 2011. Hydraulic adjustments underlying drought resistance of *Pinus halepensis*. *Tree Physiology* **31**: 637–48.

Klein T, Di Matteo G, Rotenberg E, Cohen S, Yakir D. 2012. Differential ecophysiological response of a major Mediterranean pine species across a climatic climate gradient. *Tree Physiology* DOI:10.1093/treephys/tps116.

Klute A. (ed.) 1986. *Methods of Soil Analysis, Part 1. Physical and Mineralogical Methods. Agronomy Monograph No. 9*. American Society of Agronomy/Soil Science Society of America: Madison, WI.

Li Y, Fuchs M, Cohen S, Wallach R. 2002. Water uptake profile response of corn to soil moisture depletion. *Plant, Cell & Environment* **25**: 491–500.

Marshall TJ. 1947. Mechanical composition of soil in relation to field descriptions of texture. Council for Scientific and Industrial Research, Bulletin No. 224, Melbourne.

Martin EV. 1940. Effect of soil moisture on growth and transpiration in *Helianthus annuus*. *Plant Physiology* **15**: 449–66.

Maseyk K, Lin T, Rotenberg E, Grünzweig JM, Schwartz A, Yakir D. 2008. Physiology-phenology interactions in a productive semi-arid pine forest. *New Phytologist* **178**: 603–16.

Matula S, Spongrova K. 2007. Pedotransfer function application for estimation of soil hydrophysical properties using parametric methods. *Plant Soil and Environment* **53**: 149–57.

Mickovski SB, Ennos AR. 2003. Anchorage and asymmetry in the root system of *Pinus peuce*. *Silva Fennica* **37**: 161–173.

Miller PC.1982. Nutrients and water relations in Mediterranean-type ecosystems. Presented at the Symposium on Dynamics and Management of Mediterranean-type ecosystems, June 22–26 1981, San Diego, California, USA.

Nadezhdina N, Cermak J, Gasparek J, Nadezhdin V, Prax A. 2006. Vertical and horizontal water redistribution in Norway spruce (*Picea abies*) roots in the Moravian Upland. *Tree Physiology* **26**: 1277–1288.

Nadezhdina N, Ferreira MI, Silva R, Pacheco CA. 2007. Seasonal variation of water uptake of a *Quercus suber* tree in Central Portugal. *Plant and Soil* **305**: 105–119.

Ogee J, Brunet Y, Loustau D, Berbigier P, Delzon S. 2003. MuSICA, a CO2, water and energy multilayer, multileaf pine forest model: evaluation from hourly to yearly time scales and sensitivity analysis. *Global Change Biology* **9**: 697–717.

Ogee J, Barbour MM, Wingate L, Bert D, Bosc A, Stievenard M, Lambrot C, Pierre M, Bariac T, Loustau D, Dewar RC. 2009. A single-substrate model to interpret intra-annual stable isotope signals in tree-ring cellulose. *Plant, Cell & Environment* **32**: 1071–1090.

Oren R, Ewers BE, Todd P, Phillips N, Katul G. 1998. Water balance delineates the soil layer in which moisture affects canopy conductance. *Ecological Applications* **8**: 990–1002.

Paruelo JM, Sala OE, Beltran AB. 2000. Long-term dynamics of water and carbon in semi-arid ecosystems: a gradient analysis in the Patagonian steppe. *Plant Ecology* **150**: 133–43.

Phillips DL, Gregg JW. 2003. Source partitioning using stable isotopes: coping with too many sources. *Oecologia* **136**: 261–269.

Querejeta JI, Roldan A, Albaladejo J, Castillo V. 2001. Soil water availability improved by site preparation in a *Pinus halepensis* afforestation under semiarid climate. *Forest Ecology and Management* **149**: 115–128.

Raz-Yaseef N, Rotenberg E, Yakir D. 2010a. Effects of spatial variations in soil evaporation caused by tree shading on water flux partitioning in a semi-arid pine forest. *Agricultural and Forest Meteorology* **150**: 151–62.

Raz-Yaseef, N, Yakir D, Rotenberg E, Schiller G, Cohen S. 2010b. Ecohydrology of a semi-arid forest: partitioning among water balance components and its implications for predicted precipitation changes. *Ecohydrology* **3**: 143–54.

Raz-Yaseef N, Yakir D, Schiller G, Cohen S. 2012. Dynamics of evapotranspiration partitioning in a semi-arid forest as affected by temporal rainfall patterns. *Agricultural and Forest Meteorology* **157**: 77–85.

Reid JO, Hashim O, Gallagher JN. 1984. Relations between available and extractable soil water and evapotranspiration from a bean crop. *Agricultural Water Management* **9**: 193–209.

Ritchie JT. 1974. Atmospheric and soil water influences on the plant water balance. *Agricultural Meteorology* **14**: 183–98.

Ritchie, JT. 1981. Water dynamics in the soil-plant-atmosphere system. *Plant and Soil* **58**: 81–69.

Ritter A, Munoz-Carpena R, Regalado CM, Vanclooster M, Lambot S. 2004. Analysis of alternative measurement strategies for the inverse optimization of the hydraulic properties of a volcanic soil. *Journal of Hydrology* **295**: 124–39.

Roberts J. 1983. Forest transpiration: a conservative hydrological process? *Journal of Hydrology* **66**: 133–41.

Robertson MJ, Fukai S. 1994. Comparison of water extraction models for grain soghum under continuous soil drying. *Field Crops Research* **36**: 145–60.

Rotenberg E, Yakir D. 2010. Contribution of semi-arid forests to the climate system. *Science* **327**: 451–4.

Schiller G, Atzmon N. 2009. Performance of Aleppo pine (*Pinus halepensis*) provenances grown at the edge of the Negev desert: a review. *Journal of Arid Environments* **73**: 1051–7.

Schwarzel K, Menzer A, Clausnitzer F, Spank U, Hantzschel J, Grunwald T, Kostner B, Bernhofer C, Feger K-H. 2009. Soil water content measurements deliver reliable estimates of water fluxes: a comparative study in a beech and a spruce stand in the Tharandat forest (Saxony, Germany). *Agricultural and Forest Meteorology* **149**: 1994–2006.

Shachnovich Y, Berliner PR, Bar P. 2008. Rainfall interception and spatial distribution of throughfall in a pine forest planted in an arid zone. *Journal of Hydrology* **349**: 168–177.

Sinclair TR, Ludlow MM. 1986. Influence of soil water supply on the plant water balance of four tropical grain legumes. *Australian Journal of Plant Physiology* **13**: 329–41.

Siqueira M, Katul G, Porporato A. 2008. Onset of water stress, hysteresis in plant conductance, and hydraulic lift: scaling soil water dynamics from millimeters to meters. *Water Resources Research* **44**: 1–14.

Sperry JS, Adler FR, Campbell GS, Comstock JP. 1998. Limitation of plant water use by rhizosphere and xylem conductance: results form a model. *Plant, Cell & Environment* **21**: 347–359.

Sprintsin M, Cohen S, Maseyk K, Rotenberg E, Grunzweig JM, Karnieli A, Berliner PR, Yakir D. 2011. Long term and seasonal courses of leaf area index in a semi-arid forest plantation. *Agricultural and Forest Meteorology* **151**: 565–574.

Steppe K, De Pauw DJW, Doody TM, Teskey RO. 2010. A comparison of sap flux density using thermal dissipation, heat pulse velocity and heat field deformation methods. *Agricultural and Forest Meteorology* **150**: 1046–56.

Tardieu F, Simonneau T. 1998. Variability among species of stomatal control under fluctuating soil water status and evaporative demand: modelling isohydric and anisohydric behaviours. *Journal of Experiment Botany* **49**: 419–432.

Taylor JR. 1997. *An Introduction to Error Analysis*. University Science Books: California.

Van Beek LPH, Wint J, Cammeraat LH, Edwards JP. 2005. Observation and simulation of root reinforcement on abandoned Mediterranean slopes. *Plant and Soil* **278**: 55–74.

Van Genuchten MT, Leij FJ, Yates SR. 1991. The RETC code for quantifying the hydraulic functions of unsaturated soils. Report No. EPA/600/2-91/065 RS Kerr Environmental Research Laboratory, US Environmental Protection Agency.

Veihmeyer FJ. 1956. Soil moisture. In *Encyclopedia of Plant Physiology. III. Water relations of plants*. Springer: Berlin; 64–123.

Walker CD, Brunel JP. 1990. Examining evapotranspiration in a semi-arid region using stable isotopes of hydrogen and oxygen. *Journal of Hydrology* **118**: 55–75.

Wang XF, Yakir D. 2000. Using stable isotopes of water in evapotranspiration studies. *Hydrological Processes* **14**: 1407–1421.

Warren JM, Meinzer FC, Brooks JR, Domec JC. 2005. Vertical stratification of soil water storage and release dynamics in Pacific Northwest coniferous forests. *Agricultural and Forest Meteorology* **130**: 39–58.

Williams M, Rastetter EB, Fernandes DN, Goulden ML, Wofsy SC, Shaver GR, Melillo JM, Munger JW, Fan S-M, Nadelhoffer KJ. 1996. Modelling the soil-plant-atmosphere continuum in a *Quercus-Acer* stand in Harvard forest: the regulation of stomatal conductance by light, nitrogen and soil/plant hydraulic properties. *Plant, Cell & Environment* **19**: 911–927.

Woesten JHM, Finke PA, Jansen MJW. 1994. Comparison of class and continuous pedotransfer functions to generate soil hydraulic characteristics. *Geoderma* **66**: 227–37.

Yates SR, van Genuchten MT, Warrick AW, Leij FJ. 1992. Analysis of measured, predicted, and estimated hydraulic conductivity using the RETC computer program. *Soil Science Society of America Journal* **56**: 347–54.

Zeppel M, Macinnis-Ng CMO, Ford CR, Eamus D. 2008. The response of sap flow fluxes to pulses of rain in a temperate Australian woodland. *Plant and Soil* **305**: 121–30.

Zimmermann U, Munnich KO, Roether W, Kreutz W, Schubach K, Siegel O. 1966. Tracers determine movement of soil moisture and evapotranspiration. *Science* **152**: 346–347.

